Jurnal Fisika 15 (2) (2025) 51-65
Jurnal Fisika
https://journal.unnes.ac.id/nju/index.php/jf/index

Synthesis of Carbon Quantum Dots and Their Optical Properties Under Various Conditions

Surendra Hangsarumba, Raman Kumar Kamat, Kishori Yadava, Suresh Prasad Gupta, Saddam Husain Dhobi*

Department of Physics, Patan Multiple Campus, Tribhuvan University, Patandhoka, Lalitpur-44700, Nepal

Article Info

Article History:

Received:
03 September 2025

Accepted:
23 November 2025

Published:
24 November 2025

Keywords: Carbon quantum dots, fluorescence intensity, sugar solutions, temperature effects, UV treatment, absorbance, optoelectronics.

Abstract

Carbon quantum dots (CQDs) are nanomaterials that possess great optical properties, and they hold potential for being used in biosensing, imaging, and optoelectronics. The aim of this work is to synthesis, characterization and study the optical properties of CQDs under various condition. In the present work, CQDs have been prepared by mixing equal amount (citric acid and urea) and heating in microwave at 165 °C-180 oC for 2 min to obtained dark brown color. The dark brown power was characterizations using FTIR to confirmed the different functional groups such as –P–O, –S–O, –O–C, C=C C=N and CH2/CH3 (oxygenated-, nitrogenated- and aromatic-types), while XRD analysis indicated the valuable crystalline organic phases with heterogeneous functionality features. The optical properties were carried out in water and sugar solutions (100–155mg/dl) as function of CQDs concentration, temperature, frequency and UV activation times using a Theremino spectrometer. The fluorescence intensity was enhanced with the increase of citric acid and was quenched by urea. In sugar at higher CQD concentrations, intensity was decreased from molecular trapping and light scattering. The fluorescence intensity exhibited fluctuations in water during 60s with red and blue-shifts, and the maximum peak was at 545 nm. The intensity increased with decreasing CQD: water ratio and decreased at higher concentrations, because of absorption and scattering. The temperature and frequency have strong effects on the optical responses; the higher temperatures (58 °C) promote dispersed aggregates in finer particles which leads to more light transmission in addition to larger absorption values at higher frequencies. This demonstrated the tunable features of CQDs optical properties and might give suggestions for subsequent optimization for their applications in biosensing, imaging, and optoelectronics.

✉ Correspondence address:
Tribhuvan University, Patandhoka, Lalitpur-44700, Nepal
E-mail: saddamdhobe@gmail.com

p-ISSN 2088-1509

INTRODUCTION

The unique optical and biocompatible properties of CQDs have emerged as an attractive class of nanomaterials with broad applications in bioimaging, sensing, catalysis and optoelectronics (Li et al., 2012). These zero dimensional, less than 10 nm sized carbon materials demonstrate tunable photoluminescence (PL), high quantum yield and superior photostability and are thus promising inorganic NP alternatives to conventional semiconductor QDs (Wang & Hu, 2014). There are several routes for the synthesis of CQD such as top-down (laser ablation, electrochemical oxidation) and bottom-up methods (hydrothermal, assisted microwave) that have been described days by Zhu et al. (2015). All these approaches have their own characteristic advantages in tuning the size, functionalization on surface and scale-up that considerably impact the optical properties of CQDs.

The optical properties of CQDs, particularly their PL, depend heavily on the synthesis details such as precursor used for the synthesis (Lan et al., 2016), reaction temperature and pH (Kauffmann et al., 2018) and heteroatom doping (Hartmann et al., 2019b). It is reported that nitrogen doping could enhance the PL intensity of CNs and induce a redshift by introducing extra energy states in the band gap (Zhang et al., 2015). The functional group such as carboxyl, hydroxyl and amine groups are also responsible for the optical responses of CQDs and their absorption in the surrounding medium (Xu et al., 2004). Different preparation methods, including solid-phase and solution-phase synthesis, have different effects on photoluminescence intensity and quantum yield. For instance, for one-step glucose derived solid phase prepared:100 g CQDs (343 nm) showed a product yield around 78%, with quantum yield of 6.21% (Ren et al., 2024), tricolor CQDs from dandelion precursors have quantum yields of 43.8%–32.9%–48.1%, that is, for blue – green - orange colored emission bands respectively (Long et al., 2024). Further treatments, for laser ablation and hydrothermal followed by the modification of CQD shape and optical properties (Kong et al., 2024).

CQDs possess factors associated with remarkable photostability and low cytotoxicity, paving the way for their broad applications in bioimaging and sensing (Etefa et al., 2024). Their properties are usually studied by UV-Vis spectra, PL measurements, and atomic force microscopy (Mozdbar et al., 2018). The bandgap, absorbance and PL features of the NPs are strongly sensitive to synthesis parameters such as microwave irradiation time (Kumar et al., 2020). Beyond biomedicine, the role of CQDs is extended into drug delivery (Yang et al., 2023) and cancer diagnostics (Kumar et al., 2020), organic solar cell efficiency enhancement.

In this work, we comprehensively studied CQDs under thermal, optical and frequency-modulated operation to identify the stability, trapping process and applicability in sugar sensing/preservation technologies. Furthermore, the effects of laser irradiation on the photon trapping properties of CQDs are also exposed by characterizing their photostability and photobleaching upon pulsed-laser excitation. Additionally, investigation of CQDs under frequency-modulated excitation reveals modulation-dependent responses that enable us to stabilize the structure and characterization of CQDs with strong photophysical properties. Combined, these new approaches arrive at a framework such that thermal–optical modulation not only retains CQD properties but also enables new opportunities in sensing, stabilization, laser trapping and programming of the CQD material.

METHOD

Quantum dot Preparation

Various concentrations of citric acid (Sisco Research Laboratories; 99% purity) and urea-dammor were freshly prepared separately. The amounts of citric acid and urea were weighed as required by the digital weighing machine. An aliquot of the measured quantities were then transferred to borosilicate test tube (capacity: 15 ml) for sample preparation. The resulting mixture was then heated in a Sharp microwave oven (1100 W) at 165°C -180 oC for 2 minutes. This wafer

was then heated until a brown color. After the desired color was reached, hot specimen was naturally cooled. Then, 10 ml of deionized water was added to prepare the initial solution. This solution was poured in a 100 mL beaker and the test tube was rinsed by distilled water. The wash water was also collected into the 100 ml beaker so as not to lose the sample. The mixture was further diluted to 70 ml and sonicated (180W, FSF-030S) for 30 min to afford well-dispersion. The solution was filtered after sonication, and the filtrate referred to as the sample stock solution in figure 1. For additional purification, the sample volume required was centrifuged at 6000 rpm for 2 min (REMI, Model: RM-12C). The ultimate quantum dot solution after centrifugation was prepared, and its optical property of different states were characterized.

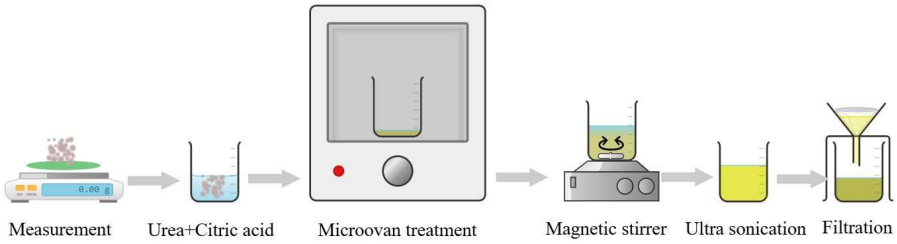

Figure 1. Experimental setup for preparation of quantum dots

Sugar solution Preparation

Three kinds of sugar solutions with 100, 120 and 140 mg/dl were prepared from the white granulated-sugar powder (greater than 99%) by dissolving it in distilled water. Sugar was weighed using a digital balance and then placed in a 500 mL borosilicate beaker. For sugar dissolution, 100 mL of distilled water was incorporated and stirred through a magnetic stirrer for 30 min. The solution was then sonicated for 10 minutes to improve the uniform dispersion. The solution was then filtered after sonication (1A Filter Water). The filtrated sugar solution was then available for testing with other agents (quantum dots and medicine) and under different conditions.

Characterization of optical properties of prepared sample

The optical spectroscopy characterization of synthesized QDs was carried out with the in-house built Theremino spectrometer (the visible range). This spectrometer allows one to study the absorption and emission properties of the quantum dots, thus allowing to gain insight into their optical behavior. The Theremino spectrometer (Dhobi et al., 2024; 2023 & Karki et al., 2021a; 2021b) is shown in figure 2. The system utilizes the Theremino_Spectrometer_V4. 0 software tool (data acquisition, spectral analysis and calibration). This program makes it possible to accurately measure the optical properties of these quantum dots.

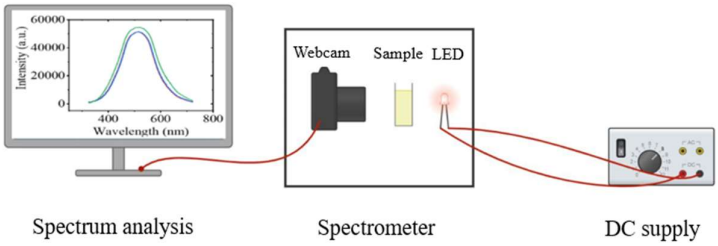

Figure 2. Experimental setup of Theremino Spectrometer (Paudel et al., 2022; Dhobi et al., 2022a; 2022b) to study the optical properties

RESULTS AND DISCUSSION

The FTIR spectrum of CQDs is presented in Figure 3(a) and Table 1. The absorption peak present in the FTIR spectra confirms the existence of functional groups needed for their optical or sensing behaviors. The absorption peak at 641.24 cm^{-1} was attributed to –P–O, –S–O, aromatic –CH or silicate-related vibrations which is consistent with its reported values at 474.68-661.77 cm^{-1} (Mansour et al., 2022). A peak at 1177.18 cm^{-1} is assigned to –O–C linkages of organic phosphate groups, which shows that the carbon matrix underwent some degree of oxidation and structural polymerization. C=C stretching mode, observed at 1721.05cm^{-1} (which supported between 1546.33 and 1656.51 cm^{-1} in previous findings), indicates the presence of conjugation π-domains, leading to electron delocalization. The presence of nitrogen is confirmed by C=N stretching vibration at 1585.43 cm^{-1} which is consistent with that reported by Mousa et al. (2023) and the band at 2938.71 cm^{-1} is assigned to asymmetrical stretching of CH_3 and symmetrical stretching of CH_2, suggesting the existence of aliphatic carbon chains. Their synergistic functional groups collectively contribute to high polarity and electron-donating ability as well as strong interaction sites with analytes, all of which are responsible for the enhancement in both charge transfer and sensing efficiency.

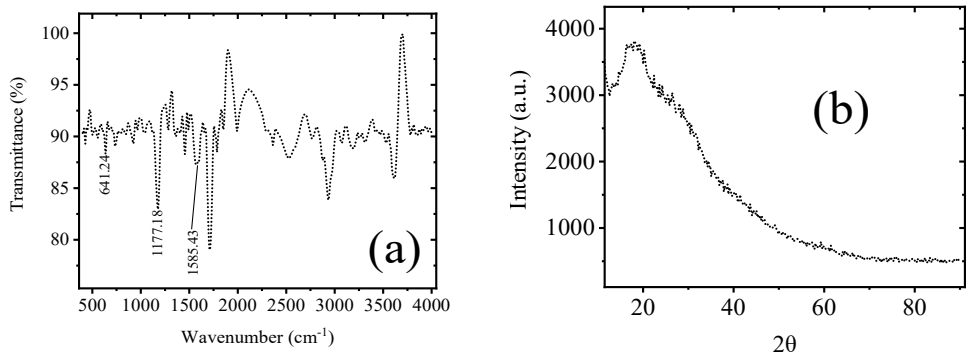

Figure 3. Characterization of CQDs (a) FTIR analysis and (b) XRD analysis

The XRD pattern of the fabricated CQDs is shown figure 3(b) and it has organic crystalline phases, including peaks around 20 o is shows the highly dispersion of carbon atom (Teng et al., 2014). The nitrogen doping derived from the urea-doped citric acid precursor promotes π-conjugation efficiencies and introduces defect sites, which are beneficial in obtaining semiconducting nature and enhancing the carrier mobility (Mansour et al., 2022). These structural architectures benefit the high efficiency charge transport and interaction with external stimuli, which leads to strong and stable sensor response. The FTIR and XRD data also support a functionally variegated but heterogeneous nature of the prepared CQDs with oxygenated, nitrogenated and aromatic zones. The above chemical diversity has found to obtain higher optical responsiveness, excitation-dependent emission, and superior adsorption ability for optical and electrochemical sensing applications preferable. The synergy between conjugated π-systems, nitrogen-dominant defect states, and aliphatic flexibility enables the CQDs to achieve highly-responsive detection toward changes in signal intensity/strength, temperature difference and analyte concentration, making the developed devices a possible competitive transduction material for future sensing gadgets.

Table 1. Experimental and referenced FTIR peak analysis

Possible assignment	Observed wavenumber (cm^{-1})	Reference wavenumber (cm^{-1})	Refrence
–P–O, –S–O, and aromatic – CH stretching or Silicate	641.24	474.68-661.77	
–O–C links of the organic phosphate groups	1177.18	1242.68	
C=C stretching	1721.05	1546.33,1656.51 3279.90	(Mansour et al., 2022)
Asymmetric CH3 & symmetric CH2 stretching	2938.71	2854.48	

The recorded results for the variation of optical intensity against the wavelength at 100 mg/dl,125 mg/dl and 155 mg/dl were shown in Figure 4(a), (b) and (c). Throughout these three cases, there is a common trend that all the light intensities decrease with an increase of CQDs concentration in sugar solutions, suggesting that CQDs have an intimate interaction with sugar molecules. This behaviour can be supported by FTIR results (Mansour et al., 2022; Mousa et aI., 2023) in which functional groups such as -P-O, -S-O, O-C, C=C, C=N and CH_2/CH_3 offer high polarity and active binding sites on the for CQDs to interact with hydroxyl-rich sugar molecules through hydrogen bonding or dipole interactions. The intensity is unchanged with 0.5 ml of CQDs for sugar concentration of 100 and 155 mg/dl (low and higher) but, with increase in the volume of CQD results in a significant reduction in intensity at this wavelength. This decrease indicated the assembly of colloids and/or more sugar adsorption on CQD which lead to greater optical scattering and absorption. Qiao et al. (2016) who had observed little variation in the PL from QD with ZnO-QDs concentration using aqueous dilution, whereas a significantly more pronounced effect is found here when varying CQDs concentrations in sugary matrices. The maximum consistently shifts around 500–600 nm and sharpens with increasing the CQD concentration, indicating variations in local micro-environment, scattering behavior, and interaction strength of CQDs with sugar molecules.

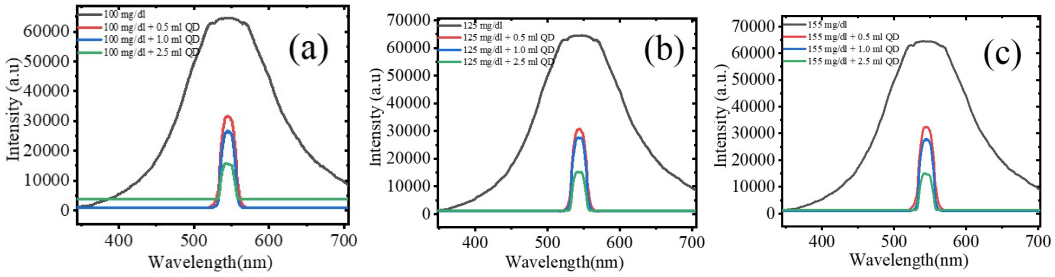

Figure 4. Impact of sugar on CQDs (a) 100mg/dl, (b) 125 mg/dl and (c) 155 mg/dl

The decrease of intensity might be due to the interactions occurring between sugar molecules and CQDs mediated by the functional groups, as listed in the FTIR analysis. The latter functions furnish polar sites and hydrogen bonding ability, which are responsible for sugar molecules binding at surface which causing a larger particle size, then forming heavier colloidal complex. This broadening increases light absorption and scattering; consequently, the transmitted intensity is with strong fall especially for higher CQD and sugar concentrations taking place at maximum number of surface interactions. In addition, an enhancement in the fluorescence intensity with increasing citric acid concentration is observed (figure 5), implying interaction of it with oxygen- and nitrogen-containing species on the CQDs, which can facilitate efficient exciton recombination. On the other hand, urea could quench the emission spectra presumably due to its interaction with such groups which block

ET pathways. Strong emission peak is only located at about 500–600 nm, which agrees with the FTIR measured Dai et al.'s study. (2015), which intersects with another peak of them at around 470 nm for the carbon QDs coated on CdTe QDs.

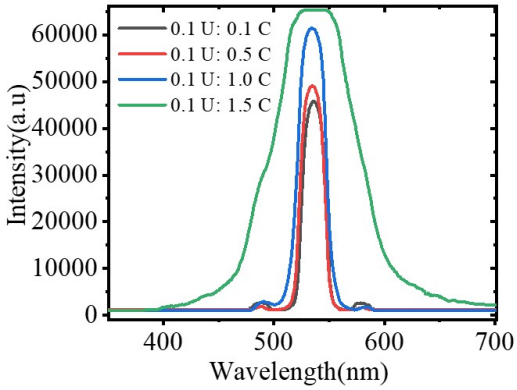

Figure 5. Impact of urea and citric acid ratio on optical properties of CQD with UV treatment

Figure 6, the time-dependent interaction of CQDs with water generating its optical response; readings were made after 30 sec, 45 sec and 60 sec laser treatment. As the CQDs were dispersed and interacted with the incident light, fluorescence intensity changes were observed around the peak wavelength (545 nm) both in Bathochromic direction (red shifts) as well as Hypsochromic direction (shorter wavelength blue shift). These changes in spectral position can be associated with functional groups which revealed by FTIR analysis, including –O–C, C=N, C=C and –P–O (Mansour et al., 2022; Mousa et al., 2023), that could engage in a strong hydrogen-bonding donating/accepting properties and attractive dipole interactions with water molecules. These polar and conjugated dyes absorb light efficiently, re-emit as fluorescence but also temporarily change the local electronic environment which leads to a shift in wavelength. This was interpreted in terms of the competition between solvation and hydrogen-bond interactions, together with electron delocalization throughout the CQDs indicating that surface chemistry is directly responsible for controlling optical responses in aqueous media.

The Bathochromic effect indicates that the CQDs excited state would be stabilized by interactions with water molecules. This stabilization led to a redshift in the emitted light. On the contrary, the hypsochromic effect shows that the excited state is more unstable so that it moves to shorter wavelengths. These variations in peak position can be attributed to the fluorescence behaviour of CQDs that absorb and re-emit light under the influence of its environment.

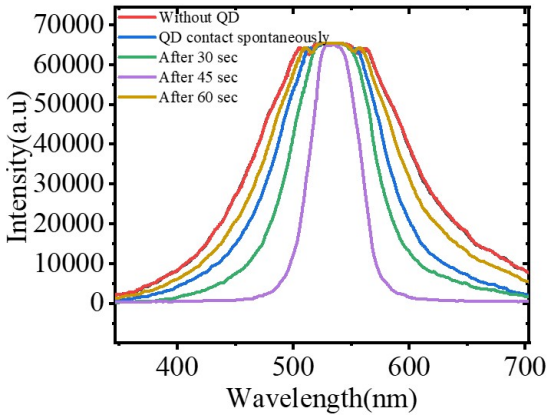

Figure 6. Impact of CQDs on water at instant contact and times passes spontaneously

The experimentally observed fluorescence change indicates how the CQDs are responsive to their surrounding aqueous environment. Upon being well dispersed in water, the CQDs serve as the solvent molecules via their functional groups. These interactions alter the local electronic structure, which accounts for dynamic changes in emission intensity and wavelength around a stable peak at 545 nm. Both Bathochromic and Hypsochromic shifts were observed thereby indicating the effect of water molecules on a competition between electron delocalization and hydrogen bonding at CQD. Time-dependent measurements also show that CQDs continue to evolve optically in the process of dispersing and reaching equilibrium with the water about them, which indicates that energy absorption and photon emission processes are ongoing. This fluorescence dynamic modulation demonstrates that CQDs are tunable optical probes whose emission characteristics can be controlled by the surrounding media. This behavior highlights the importance of surface chemistry in dictating CQD photophysics and awaits exploitation of their utility for aqueous sensing, imaging, and similar fluorescence enabled technologies.

Figure 7 shows the variation of light intensity with the volume ratio of water to CQDs covering effect of CQD on water. The behavior of the intensity with respect to volume ratio of water as compared with CQDs are. Packaging is also constant at wavelength 545nm. The comparison results are relatively weak, while the ratio of CQDs to water is 1:1 in volume. When the sample is diluted more (Higher water ratio than before), a great amount of light can transmitted through the sample. At low dilution levels (high CQD concentration) the CQDs interact more and stronger with the incoming light, resulting in higher absorbance. On the other hand, with increasing water volume and more dilute CQDs, the interaction between CQDs and incident light is weakened. This lower interaction, will give more intensity to be measured as a result of light passing through the sample.

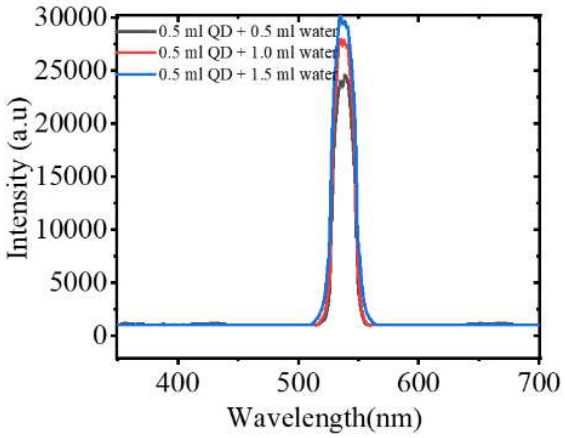

Figure 7. Optical properties of CQD with dilution

This behavior is in line with the light absorption of colloidal. In high concentration, CQDs act as efficient light absorbers owing to their dense packing of short distance. This decreases the quantity of light that will be able to cross in the sample. On the other hand, with further dilution of CQDs by water, their density should decrease and distance between the neighbouring CQDs should be widened. Conjugated C=C domains facilitate electron delocalization, which leads to absorption at select wavelengths, whereas aliphatic CH_2/CH_3 units provide steric interactions that impact interparticle distance and colloid stability. The increased effective interparticle separation with dilution results in lower aggregation (and thus scattering) and therefore, higher light transmission resulting in a radiative intensity increase. These results reveal that the functional groups not only determine the chemical reactivity and binding selectivity of CQDs, but also are able to directly control their macroscopic properties of light emission and transmission in colloidal physics.

The figure 8 indicate that except for noise the emission peak of CQDs is centered at 545 nm, whereas frequency is a decisive factor influencing optical response of CQDs. At lower frequencies the oscillations of the CQDs have a weaker intensity, leading to lower interaction with incoming light and hence higher transmission and detected intensity at 545 nm peak. At higher frequencies, however, the CQDs can oscillate more strongly and interact with incoming photons more effectively, leading to increased absorption and scattering, even though the peak wavelength may not shift, enabling a reduced overall transmitted intensity. Such a frequency-dependent intensity-modulated peak position remains well whereas the LPE peak is varied, indicating that frequency can be a good control parameter for the CQD–light interaction without affecting their inherent emission nature, which holds promising implications in optoelectronic device/sensor/light-modulation devices.

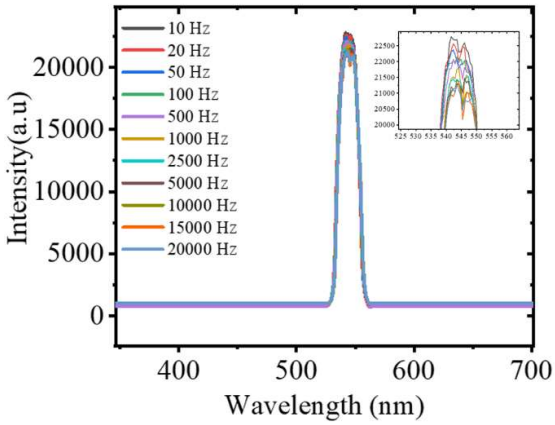

Figure 8. Impact of frequency on CQDs

The frequency dependence of the oscillation dynamics of functional groups of CQDs. At lower frequencies, the CQDs oscillate slowly and their polar groups are weakly effected by the incident light. At higher frequency, stronger oscillations make the interactions between photonic and CQDs more profound for incident light, while groups contribute to the absorption and scattering via dipolar interactions and electron delocalizations lowering transmitted intensity. The frequency-selective tuning of the optical properties. The chemical functionality provided by the CQD surface offer interesting opportunities for applications. In opto-electronics, frequency modulation allows one to tune emission and absorption properties which are key for improved light sources and detectors. In sensing, frequency dependent behavior may be useful to enhance sensitivity to certain wavelengths while in light modulation these interactions. This optical switching and modulating, revealing how both physical dynamics as well as surface chemistry dominate CQD optical performance.

Figure 9 shows that the temperature effect on the optical behavior of CQDs. These observations indicate the tunable light intensity transmitted through the CQD sample at different temperature. This suggests that the interaction between incident light and CQDs is greatly influenced by temperature. At 58 °C (higher temperature), the light intensity reaches its maximum with the finer CQD clusters being formed. On the other hand, with a lowering of temperature, it is likely that CQDs aggregate into larger clusters. These bigger clusters contribute more to the absorption and scattering due to the stronger interaction with incident light. This increased interaction means that less light is transmitted through the sample and can thus be detected with a smaller intensity. The normalized intensity of chitosan CQDs at different temperatures was studied (Sonsin et al., 2021), who observed a peak between 630 and 660 nm with slight variations in intensity. A similar intensity pattern was obtained in this study.

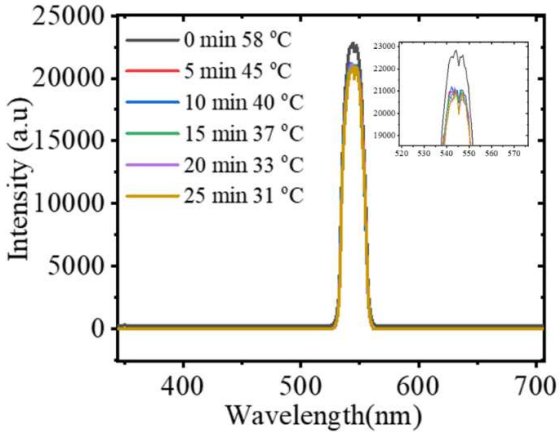

Figure 9. Impact of time and temperature on optical properties of CQDs

At higher temperatures, formation of big CQD aggregates and makes smaller, more separated clusters. This diminished aggregation is associated to less contact with incident light, and therefore permits higher transmittance through CQDs solution. At lower temperatures, when CQDs form larger clusters with stronger coupling to incident light, absorption increases and transmitted intensity decreases. At the same time, CQDs oscillation is slightly enhanced at the peak of low frequency range; polar functional groups respond less to light and act more like absorption medium for higher intensity chemical transfer. To understand qualitatively such temperature dependent and frequency sensitive behaviour, controlled by a dynamical precursor of the cluster at higher temperature. The functional groups assisted both inter-cluster dynamics and optical response which can be very crucial for many applications like optoelectronic devices environment etc.

The observed in figure 10 represents the influence of sugar concentration on optical behavior of CQDs solutions interacting with light. The observations reveal that lower sugar concentrations (100 mg/dl) result in higher light intensity, while higher sugar concentrations (155 mg/dl) lead to lower intensity, but the peak is consistent at around 545nm. The higher concentrations increase light absorption meaning less transmissible lighting. For lower sugar (100 mg/dl) concentration, the sugar molecules less interact with the incident light. The light passes through the solution with less absorption, hence higher intensity. At higher sugar concentration (155 mg/dl), larger density of the sugar molecules comes into existence and interacts more strongly with incident light. This stronger interaction contributes to more absorption and scattering of the light, thus weakness the out-going light intensity penetrating in water.

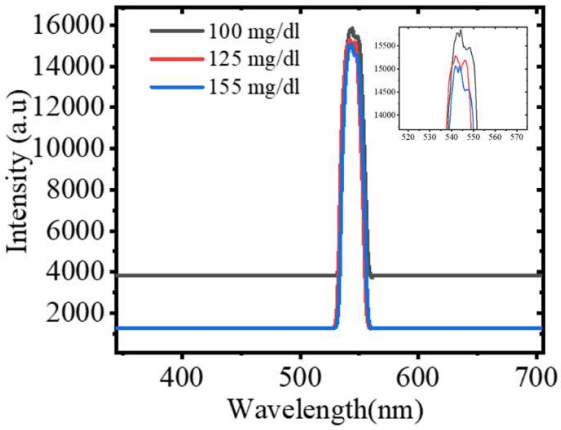

Figure 10. Optical properties of sugar concertation

The optical properties of CQD solutions depend on the concentration and are believed to be due mostly to the functional groups of CQDs. The hydrogen bonding and dipole interactions with sugar molecules. That has an important impact on light absorption and scattering, useful for technological applications. In Figure 11, it is evident that the intensity of CQDs varies with different laser activated times but their emission peak remains stationary at around 545 nm as in previous observations. Activation time is the period during which laser irradiated CQDs experience modifications in their optical behavior. The measurements were made at 0 sec (after laser exposure), after 30 sec, and then at different time periods till saturation was achieved. The data clearly indicate a hyperbathochromic effect: there is a small bathochromic shift with aging, together with a typical behavior in terms of intensities. At 0 sec, the intensity first drops due to rapid absorption of the CQDs which causes electrons to be raised into excited states without instant photon re-emission. As the case goes on, at 30 sec, the intensity increases overall while excited electrons relax slowly to the ground state producing more photons and enhancing measured emission. This enhancement increases up to the maximum value at 600 sec, which is the optical activation time. Thereafter, the effect of laser excitation is decreased and the emission becomes steady meaning that CQDs are saturated. The well-maintained 545 nm peak and the hyperbathochromic shift and intensity variation reveal that the electronic structures of CQDs can be significantly adjusted upon activation, while its fundamental emission wavelength remains unchanged.

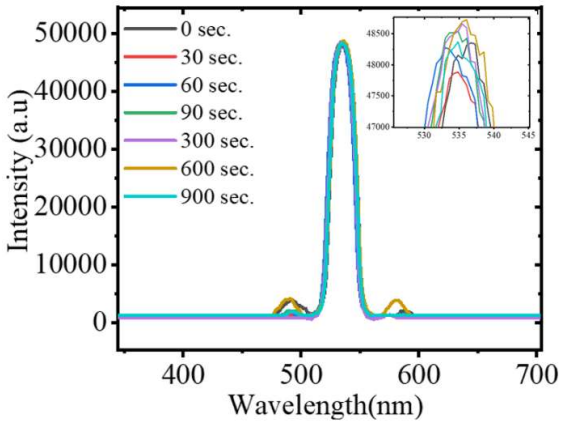

Figure 11. Laser treated CQDs at different activation time

The observed phenomena are of significance for applications of CQDs in optoelectronic, sensing, and image-related fields. For laser treated CQDs, the intensity varies with the laser activation time and decreases at first then rises to a maximum value at 600 s. Such behavior is attributed to the excitation and relaxation of CQD atoms, aided by electron-transfer process as a result of surface functional groups including –O–C, C=N, –P–O, C=C, and CH2/CH3 through hydrogen bonding and dipole interactions which can modify photon emission. The fluorescence appears as a hyperbathochromic shift to shorter wavelengths and is associated with changes in the local electronic state of the CQDs.

At a given frequency intensity is taken as that at which the peak of intensity occurs at 550 nm and fitted curve showing the variation with frequency vs internaisty is shown inf figure 12. The fitted curve shows with frequency increases intensity decays exponentially reaching to an asympotical limiting value at very high frequencies 20796.69 Hz. The value 1458.74 corresponds to the initial offset of intensity and asymptote, whereas exp(−4.01×10−4 x) determines the decay rate. The model has a high R2 = 0.99, indicating that the exponential decay function represents the elementary data very accurately

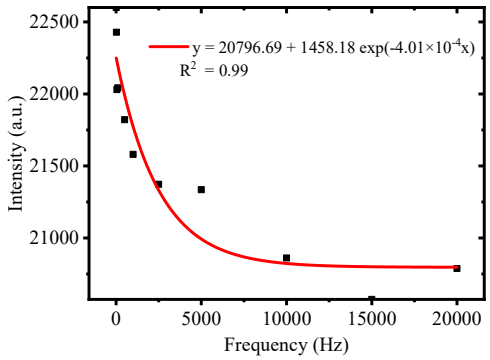

Figure 12. Fitting of intensity with frequency at 550 nm

Figure 13 is exponential decay asympote and the equation in figure 13, x is the frequency, and y is the intensity. The model predicts that at high frequency, the intensity has a decay exponent exp(−4.01×10−4x) models decay. With an R2 being rather high (R2=0.99) the model shows a strong correlation suggesting that an exponential decay function describes the experimental data fairly precisely.

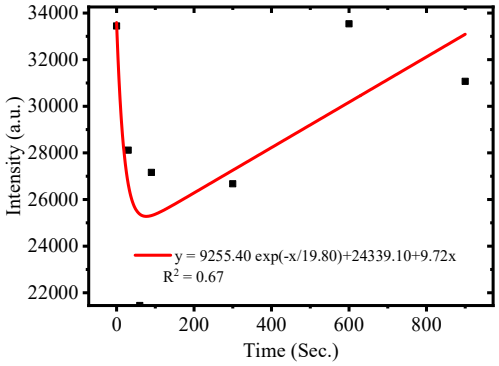

Figure 13. Fitting of intensity with time at 540 nm

Exponential-decay decay-constant decaying term as well shift, linearly increasing intensity. Originally the behavior is strong because of the exponent exp(-x/19.80) which vanishes as time goes on. In addition to that decay, a linear term, 9.72x was included which adds a constant increase in the intensity with time. And furthermore, a 24339.10 constant makes sure the intensity is never completely zero. Consequently, the model predicts that intensity initially decreases when losing strength on account of the decaying factor and eventually stabilizes and increases due to linearity. The R-square (0.66) suggests that 66% of the variation in intensity was explained by model, it indicate a moderate fitting to data.

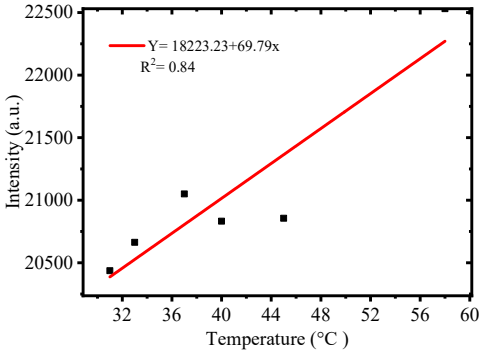

Figure 14. Fitting of intensity with time at 550 nm

The equation of the figure 14 give in show linear dependence with temperature which, indicates that with rise in the temperature intensity also goes on the increase linearly. The slope 69.79 means that if the temperature increases by one there is an increase of intensity about 69.79. The intercept 18223.23 indicates the initial intensity of zero temperature. The R2=0.84 indicates that the model also accounts for 84.3% of variation in intensity, which means that temperature and intensity have a very strong relationship in terms of positive correlation. That is to say, temperature plays an important role on the intensities, and the simple linear relationship actually describes most of the trend in data. But some other factors, measurement error and nonlinear effects not included in the model would account for 15.7% of residual variation.

CONCLUSION

In summary, in the current work, CQDs were well prepared through a facile hydrothermal treatment from citric acid and urea precursors, and their optical properties have been systematically studied with changing of conditions. The functional groups and molecular structures such as oxygenated, nitrogenated, aromatic motifs are responsible for the size-dependent fluorescence, light absorption ability and scattering behavior of the CQDs based as examined by FTIR and XRD analysis. Optical investigation of CQD interactions with sugar solutions, water, laser activation, frequency and temperature leads to the strong evidence of dynamic modulation (both Bathochromic and Hypsochromic) effects in emission intensity/wavelengths. These effects are mainly due to the existence of surface functional groups that allow H-bonding, dipole interactions and electronic delocalization, whereas environmental conditions play also an important role in the optical response. Quantitative analyses of spectral intensity as a function of frequency, time and temperature were also obtained from mathematical modeling which revealed strong correlations and expected patterns. In general, the study confirms tunable and sensitive optical properties of CQDs highlighting their promise for applications in optoelectronic devices, sensing and imaging as well as fluorescence-based technologies in which surface chemistry or environmental interactions can be exploited to maximize efficacy.

ACKNOWLEDGEMENT

The authors extend their gratitude to all faculty and non-faculty members of the Department of Physics, Patan Multiple Campus, Tribhuvan University, Patandhoka, Lalitpur, Nepal, for their support in providing a conducive research environment, essential resources, and other facilities during this study.

REFERENCE

Xu, X., Ray, R., Gu, Y., Ploehn, H. J., Gearheart, L., Raker, K., & Scrivens, W. A. (2004). Electrophoretic analysis and purification of fluorescent single-walled carbon nanotube fragments. Journal of the American Chemical Society, 126(40), 12736-12737.

Zhang, J., Yuan, Y., Liang, G., & Yu, S. H. (2015). Scale-up synthesis of fragrant nitrogen-doped carbon dots from bee pollens for bioimaging and catalysis. Advanced Science, 2(4).

Liu, M. L., Chen, B. B., Li, C. M., & Huang, C. Z. (2019). Carbon dots: synthesis, formation mechanism, fluorescence origin and sensing applications. Green chemistry, 21(3), 449-471.

Zhu, S., Song, Y., Zhao, X., Shao, J., Zhang, J., & Yang, B. (2015). The photoluminescence mechanism in carbon dots (graphene quantum dots, carbon nanodots, and polymer dots): current state and future perspective. Nano research, 8, 355-381.

Wang, Y., & Hu, A. (2014). Carbon quantum dots: synthesis, properties and applications. Journal of Materials Chemistry C, 2(34), 6921-6939.

Li, H., Kang, Z., Liu, Y., & Lee, S. T. (2012). Carbon nanodots: synthesis, properties and applications. Journal of materials chemistry, 22(46), 24230-24253.

Ren, H., Fan, Q., Feng, X., Liu, J., & Zhao, Y. (2024). Facile Synthesis of Fluorescent Carbon Quantum Dots with High Product Yield Using a Solid-Phase Strategy. Molecules, 29(22), 5317. https://doi.org/10.3390/molecules29225317

Long, X., Liao, S., Wang, J., Ma, Y., & Wu, S. (2024). Synthesis and Chromatographic Isolation of Blue, Green, and Orange Emissive Carbon Dots with High Quantum Yields from Taraxacum. Dyes and Pigments. https://doi.org/10.1016/j.dyepig.2024.112211

Kong, J., Wei, Y., Zhou, F., Zhao, S., Wan, M., & Zhang, X. (2024). Carbon Quantum Dots: Properties, Preparation, and Applications. Molecules. https://doi.org/10.3390/molecules29092002

Etefa, H. F., Tessema, A. A., & Dejene, F. B. (2024). Carbon dots for future prospects: synthesis, characterizations and recent applications: a review (2019–2023). C, 10(3), 60.

Kumar, P., Bhatt, G., Kaur, R., Dua, S., & Kapoor, A. (2020). Synthesis and modulation of the optical properties of carbon quantum dots using microwave radiation. Fullerenes, Nanotubes and Carbon Nanostructures, 28(9), 724-731.

Mozdbar, A., Nouralishahi, A., Fatemi, S., & Mirakhori, G. (2018, January). The effect of precursor on the optical properties of carbon quantum dots synthesized by hydrothermal/solvothermal method. In AIP Conference Proceedings (Vol. 1920, No. 1). AIP Publishing.

Yang, H. L., Bai, L. F., Geng, Z. R., Chen, H., Xu, L. T., Xie, Y. C., ... & Wang, X. M. (2023). Carbon quantum dots: Preparation, optical properties, and biomedical applications. Materials Today Advances, 18, 100376.

Dai, X., Wang, H., Qian, Z., Yi, Q., Wang, Y., Cong, S., ... & Zou, G. (2015). Emission switching in carbon dots coated CdTe quantum dots driving by pH dependent hetero-interactions. Applied Physics Letters, 107(20).

Qiao, B., Zhao, S., Xu, Z., & Xu, X. (2016). Synthesis of ZnO quantum dots and their agglomeration mechanisms along with emission spectra based on ageing time and temperature. Chinese Physics B, 25(9), 098102.

Sonsin, A. F., Nascimento, S. M., Albuquerque, I. M. B., Silva, E. C., Rocha, J. C. A., Oliveira, R. S., ... & Fonseca, E. J. (2021). Temperature-dependence on the optical properties of chitosan carbon dots in the solid state. RSC advances, 11(5), 2767-2773.

Mousa, M. A., Abdelrahman, H. H., Fahmy, M. A., Ebrahim, D. G., & Moustafa, A. H. (2023). Pure and doped carbon quantum dots as fluorescent probes for the detection of phenol compounds and antibiotics in aquariums. Scientific Reports, 13(1), 12863.

Mansour, A. T., Alprol, A. E., Abualnaja, K. M., El-Beltagi, H. S., Ramadan, K. M., & Ashour, M. (2022). The using of nanoparticles of microalgae in remediation of toxic dye from industrial wastewater: kinetic and isotherm studies. Materials, 15(11), 3922.

Dhobi, S. H., Nakarmi, J. J., Yadav, K., & Gupta, S. P. (2024). Magneto optical properties of atmospheric air molecules. Journal Scientific and Technical of Information Technologies, Mechanics and Optics, 155, 375–383. doi: 10.17586/2226-1494-2024-24-3-375-383

Dhobi, S. H., Nakarmi, J. J., Waiba, R., Koirala, B., Yadav, K., Gupta, S. P., & Lemle, L. D. (2023). Magneto-optical properties of water and saltwater in presence of a magnetic field. Journal of Physics: Conference Series, 2540, 012002. doi:10.1088/1742-6596/2540/1/012002

Karki, B., Dhobi, S. H., Dhobi, I., Pandey, D., & Pandey, B. K. (2021a). Study the optical properties of drinking water supply by KUKL and KVWSIP in Kathmandu Valley. Discover Water, 1, 1–13. https://doi.org/10.1007/s43832-021-00006-2

Karki, B., Dhobi, S. H., & Dhobi, I. (2021b). Optical properties of transparent liquid: Water, oils, and honey. Journal of Materials and Environmental Science, 12(12), 1524–1537. https://www.jmaterenvironsci.com/Document/vol12/vol12_N12/JMES-2021-12122-Karki.pdf

Paudel, K., Dhobi, S. H., Dahal, K., Waiba, R., Yadav, K., Narayan, K. C., & Nakarmi, J. J. (2022). Optical interaction at the boundary layer of oil–water–saltwater. International Journal of Research and Innovation in Applied Science, 7(3), 1–6. https://rsisinternational.org/journals/ijriss/Digital-Library/volume-6-issue-3/01-06.pdf

Dhobi, S. H., Khatri, U., Yadav, K., Paudel, K., Koirala, B., Nakarmi, J. J., Waiba, R., & Nepali, A. (2022). Spring drinking water optical properties (420 nm–700 nm) in hilly region near Nisi Khola area, Baglung, Nepal. Journal of Research in Engineering and Applied Sciences, 7(3), 347–355. https://doi.org/10.46565/jreas.202273347-352

Dhobi, S. H., Koirala, B., Yadav, K., Nakarmi, J. J., Gupta, S. P., Das, S. K., … Sah, R. L. (2022). Temperature influence on the optical properties, attenuation coefficient, and total molecular cross section of Dhunge Dhara drinking water. Makara Journal of Science, 26(4), 3. https://doi.org/10.7454/mss.v26i4.1335

Koirala, S., Neupane, D., Mulmi, D. D., & Dhobi, S. H. (2024). Optical properties of daily used water in Kathmandu Valley. Discover Water, 4, Article 26. https://doi.org/10.1007/s44253-024-00026-4

Teng, X., Ma, C., Ge, C., Yan, M., Yang, J., Zhang, Y., ... & Bi, H. (2014). Green synthesis of nitrogen-doped carbon dots from konjac flour with "off–on" fluorescence by Fe 3+ and L-lysine for

bioimaging. Journal of Materials Chemistry B, 2(29), 4631-4639. https://doi.org/10.1039/C4TB00368C